Coherence and quasistable states in a strong infrared field

Changchun Zhong and F. Robicheaux

Phys. Rev. A **93**, 033410 — Published 10 March 2016

DOI: 10.1103/PhysRevA.93.033410

Coherence and quasi-stable states in a strong infrared field

Changchun Zhong* and F. Robicheaux†
Department of Physics and Astronomy, Purdue University, West Lafayette IN, 47907 USA

We study the quasi-stability of UV-pulse-train-excited H atoms in a strong infrared (IR) laser as a function of the phase delay of the UV-pulse-train relative to the IR laser. The UV-pulse-train contains two frequency components. When the two components have frequencies separated by two IR photons, the population of surviving electrons is modulated by up to ten percent. When electrons are excited to right above or below the threshold, the survival probabilities have inverted phase delay dependence which can be explained classically. When the two frequencies are one IR-photon apart, the angular symmetry of the quasi-stable electrons is broken, and the asymmetry is also controlled by the phase delay. The asymmetrical distribution can be observed while the IR is on and smoothly evolves to a nonzero asymmetry that only weakly depends on the duration of the IR field.

PACS numbers: 32.80.Rm, 32.80.Wr

I. INTRODUCTION

When laser excited atoms are exposed to an intense microwave or laser field, a certain fraction will be trapped in highly excited states for a long time [1–5], leading to their classification as quasi-stable states. Classically, the electrons in quasi-stable states derive their stability through orbiting in a weakly bound trajectory where they have little chance to absorb enough energy to escape [3, 4, 6]. These quasi-stable states can be studied spectrally, and a series of survival peaks can be detected [2, 3]. These peaks are formed because electrons at the correct initial energy can reach the quasi-stable states through multi-photon transitions, while other initial energies will lead to ionization because the electron can not reach the quasi-stable state by absorbing integer number of photons.

As is well known, the properties of an excited electron wave packet in an intense IR field will differ depending on whether it was created by a single UV pulse or a train of them [7]. The properties of electrons excited by a single UV pulse are mainly determined by the IR intensity and frequencies. However, the behavior of electron wave packets produced by a UV-pulse-train is also affected by coherence, such as the large peak to peak modulation observed experimentally [7]. The coherence, timing, and varied energy of electrons could be controlled independently by changing the properties of the UV-pulse-train. A recent experiment can be seen in Ref. [8] for Li atoms in a microwave field, where they observed modulation of the population of weakly bound electrons by changing the delay in the pulse train and the detuning relative to threshold. Studying these features surely provides a novel, powerful tool to explore strong field interactions [7, 9].

In this paper, we numerically study the survival probability of H in quasi-stable states as a function of the phase delay of a UV-pulse-train relative to an intense IR laser.

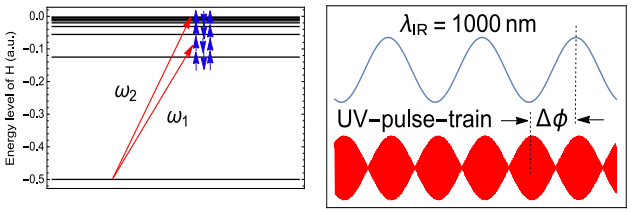

(a) (b)

FIG. 1. (Color online) **(a)** Each black line corresponds to an energy level of the H atom. The red arrows show the electron being brought to the desired states by the UV lasers. Then the electron (blue arrows) continues evolving in the presence of the intense IR field plus atomic potential. **(b)** A sketch for the UV-pulse-train and IR field, where $\omega_2 - \omega_1 = 2\omega_{IR}$. The IR laser lasts 1.6×10^4a.u. in time. $\Delta\phi$ is the phase delay of the UV with respect to the IR.

The system is similar to the experiment [8], while we replace the microwave field by an intense IR field. The UV-pulse-train is created by combining two UV lasers with frequencies ω_1 and ω_2, as shown in Fig. 1(a). The phase delay between the pulse train and the IR laser is controlled by changing the initial phase of the two UV lasers. In our simulation, the two UV lasers are treated as two separate sources of excitation due to the linearity of the Schrödinger equation. Thus, a modulation by coherence in the survival probability is expected if the surviving electrons from each source have the same quantum numbers. This is satisfied when the two UV frequencies are separated by two IR photons ($\omega_2 - \omega_1 = 2\omega_{IR}$), since the wave packets that reach the quasi-stable states will have the same even or odd parity [10]. In this case, a modulation of the population of weakly bound electrons is observed and is closely related to the phase delay. The peak to peak modulation in the survival probability varies for different launch energies. The launch energy is defined as the initial energy of electrons excited by the UV laser with frequency ω_1. When the launch energies are right above and below the threshold, the modulations are phase inverted, which is the same as the experimental

* zchangch@purdue.edu
† robichf@purdue.edu

result in Ref. [8]. When the two UV frequencies are only one IR-photon apart ($\omega_2 - \omega_1 = \omega_{IR}$), no coherence in the survival probability is seen. However, an interesting phenomenon is observed that the angular symmetry of the bound wave packet is broken and is also controlled by the phase delay. This asymmetrical distribution can be observed while the IR is on and smoothly evolves to a final value that only weakly depends on the IR duration. In the sections which follow, we introduce the numerical approach that we use, present the results and analysis, compare them to our expectations, and comment on their implications.

We use atomic units except where explicitly stated otherwise.

II. THEORY AND METHOD

In a simulation, H atoms are prepared in the ground state at the beginning. Then a weak UV-pulse-train is turned on to bring the electrons to the desired states through one-photon absorption. The UV-pulse-train is created by turning on two UV lasers with frequencies ω_1 and ω_2, as shown in Fig. 1. The beat frequency of the two lasers is assumed to be a multiple of an intense IR field so that the beats stay in phase with the IR over many cycles. After the UV pulse, the excited electrons continue to evolve in the presence of the intense IR field. The energy and angular momentum of the electrons change through multi-photon transitions. By tuning the initial phase of the UV lasers, the envelope of the UV-pulse-train can be shifted relative to the IR field. Figure 1(b) schematically shows the phase delay between the UV-pulse-train and the IR laser, where the UV frequency separation is two IR photons. In the simulation, the weak UV-pulse-train is treated as a source term in the Schrödinger equation. The duration of the pulse train should be short on the scale of the IR duration and long on the scale of one IR cycle. As long as this condition is satisfied, the actual duration of the pulse train becomes less important. In the simulation, we make the pulse train last about 4 IR cycles. The IR field lasts about 1.6×10^4a.u. and its wavelength is $1000nm$, giving the frequency $\omega_{IR} \sim 0.0455$a.u.. The IR intensity is chosen to be $\mathrm{I} = 4.256 \times 10^{12} W/cm^2$. Similar to Ref.[10], the intensity is weak in the sense of affecting the H ground state, while strong in the sense of interacting with its excited states.

The dynamics is approximately governed by the following time dependent Schrödinger equation with a source term [10],

$$i\frac{\partial \Psi_e(\vec{r},t)}{\partial t} - \tilde{H}\Psi_e(\vec{r},t) = S(\vec{r},t), \tag{1}$$

where $\Psi_e(\vec{r},t)$ is the excited wave function of the electron after absorbing one UV photon and it is initially zero everywhere before the UV-pulse-train is on. The source term is

$$\begin{aligned} S(\vec{r},t) = \{&F_{UV1}(t)\exp(-i(\omega_1 t+\sigma_1))+ \\ &F_{UV2}(t)\exp(-i(\omega_2 t+\sigma_2))\}z\Psi_g(\vec{r})\exp(-iE_g t), \end{aligned} \tag{2}$$

which provides the source of amplitude for the excited wave function. The UV lasers in the source take a Gaussian envelope, $F_{UV(1,2)}(t) \propto \exp(-t^2/2t_w^2)$ and t_w is chosen to make sure they last 4 IR periods in time. $\tilde{H}$ is the electron Hamiltonian without the UV interaction,

$$\tilde{H} = -\frac{1}{2}\nabla^2 + V(\vec{r}) - F_{\mathrm{IR}}(t)z, \tag{3}$$

where the third term is the interaction (using the dipole approximation) between the electron and the IR field (linearly polarized), and $V(r)$ is the interaction of the electron with the nucleus. $F_{\mathrm{IR}}(t)$ reads,

$$F_{\mathrm{IR}}(t) = F_m\cos(\omega_{\mathrm{IR}}t)\left(\mathrm{erf}[\frac{(t-t_i)}{t_w}] - \mathrm{erf}[\frac{(t-t_f)}{t_w}]\right). \tag{4}$$

The error function is used to smoothly turn on and off the IR laser. Noticing the linearity of Eq. 1, we can separate it into two parts, each of them treats only one UV laser. By doing this, the numerical calculation is greatly simplified. The excited wave function can be written as $\Psi_e(\vec{r},t) = \Psi_{e1}(\vec{r},t) + \Psi_{e2}(\vec{r},t)$. Thus the separated equations are

$$i\frac{\partial \Psi_{ei}(\vec{r},t)}{\partial t} - \tilde{H}\Psi_{ei}(\vec{r},t) = S_i(\vec{r},t), \tag{5}$$

in which

$$S_i(\vec{r},t) = F_{UVi}(t)z\Psi_g(\vec{r})\exp(-i(E_g t+\omega_{UVi}t+\sigma_i)). \tag{6}$$

The index $i = (1,2)$. The phase delay of the UV-pulse-train relative to the IR can be changed by tuning σ_i (the initial phase of UV lasers).

The quantum simulation is performed by numerically solving Eq. 5. Each wave function is represented on a 2D space spanned by discrete radial points and an angular momentum basis. For the radial part, we use a nonlinear square root mesh. The propagation operator is constructed using a split-operator technique of the form,

$$U(\delta t) = U_1(\frac{\delta t}{2})U_2(\delta t)U_1(\frac{\delta t}{2}), \tag{7}$$

where the approximation $U_i(\delta t) = (1 - iH_i\delta t/2)/(1 + iH_i\delta t/2)$ is used. During the time propagation, an absorbing potential is used, such that the ionized electrons are efficiently absorbed. One can refer to [11] for the details of the numerical technique. The final wave function in the quasi-stable states is obtained by adding Ψ_{e1} and Ψ_{e2}. In the sections that follow, one will see that most of the interesting effects are from the interference between these two wave packets.

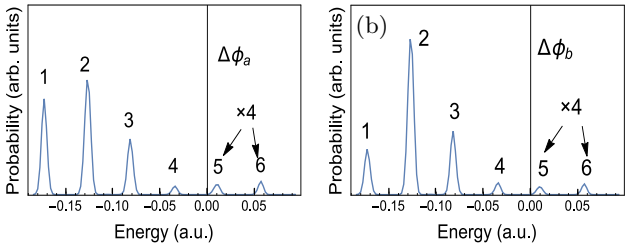

(a) (b)

FIG. 2. The survival probability in quasi-stable states (with principal quantum number $n > 6$) as a function of the launch energies. Each figure has a given phase delay between the UV-pulse-train and the IR. The digits from 1 to 6 are to label each peak close to different launch energies. The peak 5 and 6 are multiplied by 4 to make them visible. Figure 2(a) and **??** are plotted in the same scale. **(a)** The phase delay is $\Delta\phi_a = \pi/2$. **(b)** The phase delay is $\Delta\phi_b = \pi$.

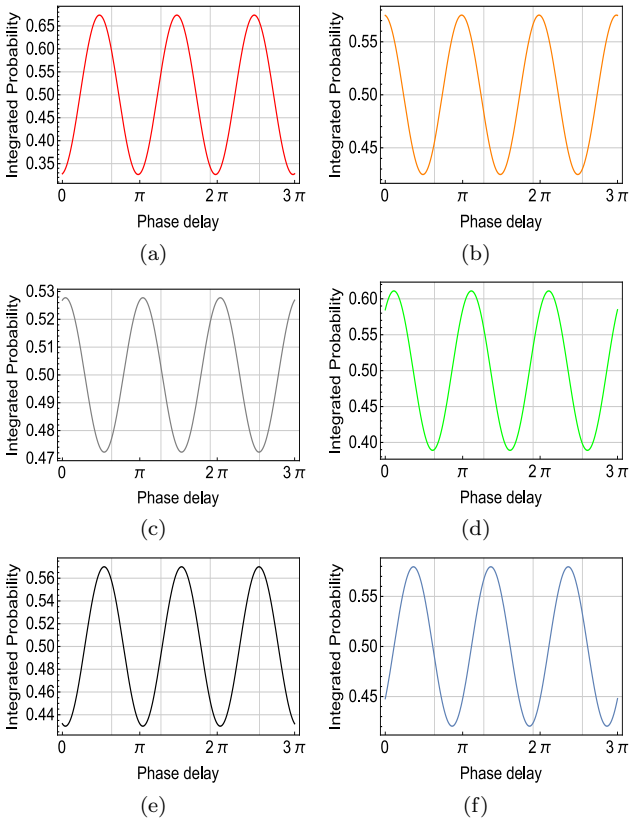

FIG. 3. (Color online) The integrated probability for each peak in Fig. 2 as a function of the phase delay of the UV-pulse-train relative to the IR. The integrated probability is obtained by integrating the survival probabilities of each peak in the spectrum of Fig. 2 and dividing it by twice its average over phase delay. The graph (a) corresponds to peak 1 in Fig. 2, (b) corresponds to peak 2 in Fig. 2, etc. All curves oscillate around 0.5. The bigger the oscillation is, the more the peak is in contrast with different phase delay.

III. RESULTS AND DISCUSSION

The UV-pulse-train is simulated by turning on two UV lasers which act as two independent sources in the system. In order to study the survival spectrum, the frequency of the first UV laser (ω_1) is scanned such that the electrons have initial energies ranging from $E = -0.17$a.u. to $E = 0.11$a.u. relative to the ionization threshold. For each frequency ω_1, the frequency of the second UV laser is tuned to satisfy $\omega_2 = \omega_1 + N * \omega_{IR}$ ($N = 1$ or 2). For each launch energy, the data is accumulated after the intense IR laser is smoothly turned off.

Refer to Eq. 5, the final wave function can be written as

$$\begin{aligned}\Psi_e(\vec{r},t) =& \Psi_{e1}(\vec{r},t) + \Psi_{e2}(\vec{r},t) \\ =& \psi_{e1}(\vec{r},t)\exp(-i\sigma_1) + \psi_{e2}(\vec{r},t)\exp(-i\sigma_2),\end{aligned} \tag{8}$$

where $\psi_{ei}(\vec{r},t)$ are the solutions to Eq. 5 when $\sigma_i = 0$ ($i = 1$ or 2). In principle, any observable $\hat{A}$ can be obtained through evaluating

$$\langle\hat{A}\rangle = \sum_{i=1}^{2}\langle\psi_{ei}|\,\hat{A}\,|\psi_{ei}\rangle + 2\mathrm{Re}\{\langle\psi_{e2}|\,\hat{A}\,|\psi_{e1}\rangle\exp(i(\sigma_2-\sigma_1))\}. \tag{9}$$

The second term shows clearly how the coherence is manifest in the value of an observable. By tuning the value of σ_i ($i = 1$ or 2), the phase delay of the UV-pulse-train relative to the IR laser will change accordingly, and so will the value of $\langle\hat{A}\rangle$. In the following subsections, observables $\hat{A} = \hat{I}$ and $\hat{A} = \cos\theta$ are discussed. They respectively correspond to the survival probability and orientation of electrons that survive the intense IR field. While the IR laser is on, the angular symmetry as a function of time is also discussed.

A. Coherence for two ω_{IR} separation

Equation 9 gives the population of survival electrons when the observable $\hat{A} = \hat{I}$. The coherence in the survival population is greatly determined by the overlap $\langle\psi_{e2}|\psi_{e1}\rangle$. Since ψ_{e1} and ψ_{e2} are the electron wave functions in the quasi-stable states, they will have similar principal quantum numbers. Moreover they tend to have even (odd) angular quantum numbers if their initial energies are odd (even) number of IR-photon's away from the threshold [10]. When the two UV lasers have frequencies separated by two IR photons (N=2), they will create two electron wave packets with initial energies separated by two IR photons. As a result, ψ_{e1} and ψ_{e2} will concurrently have either odd or even angular quantum numbers when they reach the quasi-stable states. Thus, the overlap between ψ_{e1} and ψ_{e2} becomes significant, and coherence is expected in the electron's survival probability.

Figure 2 shows the survival spectrum for two different phase delays of the UV-pulse-train relative to the IR. The

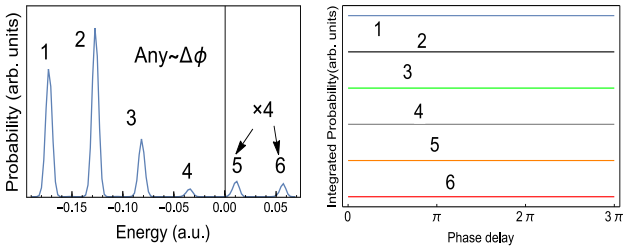

FIG. 4. (Color online) The digits are used to track each peaks. The peak 5 and 6 are multiplied by 4 to make them visible. **(a)** The survival spectrum for the two components of the UV-pulse-train being separated by one IR photon. The shape of the spectrum keeps unchanged for any phase delay. **(b)** The straight lines denote the integrated survival probability of each peak in Fig. 4(a) in terms of the phase delay. Those lines are straight because no modulation is observed in this case.

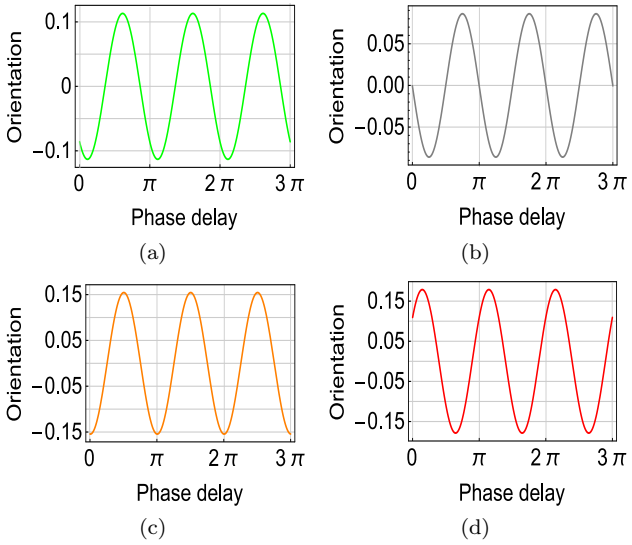

FIG. 5. (Color online) The orientation of the survival population as a function of the phase delay of the UV-pulse-train relative to the IR. The red (orange, gray, green) line is for the launch energy $E = 0.057a.u.$ ($E = 0.011a.u.$,$E = -0.034a.u.$,$E = -0.077a.u.$). Each line is oscillating periodically around zero, indicating the phase delay is controlling the angular symmetry of the survival wave packets.

equally separated train of peaks is formed by electrons trapped in the quasi-stable states, which is discussed in Ref. [2, 3, 10]. The height of the peaks in the Fig. 2(a) and **??** are quite different, indicating the level of coherence in the electron population. Continuously changing the phase delay will lead to a change in the interference term in Eq. 9. This phase sensitivity is an evidence that, after the UV excitation, most of the energy transfer from the IR to the excited electrons happens during the first few IR cycles, as suggested by the Simpleman's model [4, 5]. In order to clearly show this, for each phase delay, we integrate the survival probabilities of each peak in the spectrum and divide it by the twice average over phase delay. This quantity oscillates around 0.5, which contrast the survival probabilities of different phase delays. The result is shown in Fig. 3. Each line from 3(a) to 3(f) corresponds to each peak in Fig. 2 from the left to the right. Each curve is oscillating with a period of π in terms of phase delay. The period π is determined by the fact that the UV-pulse-train repeats itself when its envelope shifts by π. What is more, the survival probability of electrons with different launch energies have varied phase delay dependence. For those peaks right above and below the threshold, shown by the grey, green and black curves in Fig. 3, they tend to have inverted phase delay dependence, because of the fact that the ionization and recombination happens at the same time when electrons are tuned below or above the threshold. For those peaks far below the threshold, shown by the red curve, the phase delay dependence is not inverted compared to the above threshold curve, which is a topic that deserves further study.

B. Coherence for one ω_{IR} separation

When the frequencies of the two UV lasers are separated by one IR photon (N=1), although ψ_{e1} and ψ_{e2} still have similar principal quantum numbers, they will have different parity (even for one and odd for the other) [10]. Thus, the overlap $\langle\psi_{e1}|\psi_{e2}\rangle$ is expected to be zero, indicating no coherence in the survival probability. As shown in Fig. 4(a), the height of the survival peaks remains the same for any phase delay of the UV-pulse-train relative to the IR. As a result, the integrated probability for each peak will approximately be a constant, which is shown by the horizontal lines in Fig. 4(b).

However, the parity difference of the two wave packets indicates an angular symmetry broken. The angular symmetry of an electron can be evaluated by the quantity (the orientation)

$$\text{Orientation} = \frac{\langle\Psi_e(\vec{r})|\cos\theta|\Psi_e(\vec{r})\rangle}{\langle\Psi_e(\vec{r})|\Psi_e(\vec{r})\rangle}, \tag{10}$$

where θ is the polar angle. Obviously, the orientation takes the value between $[-1, 1]$, and it being larger (smaller) than zero means the electrons are distributed more at the upper (lower) half sphere. From Eq. 9, when the observable $\hat{A} = \cos\theta$, the first term will vanish because the angular integral is nonzero only if the functions in the integral have angular quantum numbers differ by one ($\Delta l = \pm 1$). So the numerator in Eq. 10 simplifies to

$$\langle\cos\theta\rangle = 2\text{Re}(\langle\psi_{e2}|\cos\theta|\psi_{e1}\rangle\exp(i(\sigma_2 - \sigma_1))). \tag{11}$$

Thus, the orientation is also phase delay dependent. Meanwhile, $\langle\psi_{e2}|\cos\theta|\psi_{e1}\rangle$ is nonzero since the two wave packets exclusively have even or odd angular quantum numbers ($l = 1, 3, 5...$ for ψ_{e1}, then $l = 2, 4, 6...$ for ψ_{e2}

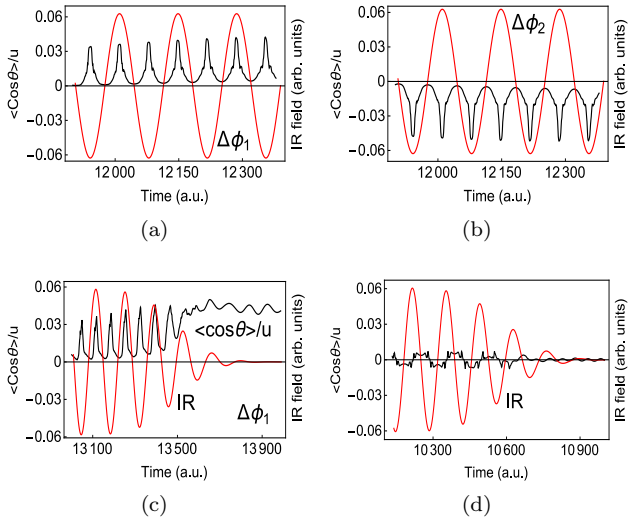

FIG. 6. (Color online) $\langle\cos\theta\rangle$ as a function of time while the IR is on (black lines). The plot is normalized by the final bound population (u= $\langle\Psi_e(\vec{r})|\Psi_e(\vec{r})\rangle$). The red curves are the IR. The launch energy $E = -0.082$a.u. and $N = 1$ for Fig. 6(a) 6(b) and 6(c). **(a)** $\Delta\phi_1 = \pi/2$. **(b)** $\Delta\phi_2 = \pi$. **(c)** The IR field is being smoothly turned off, while $\langle\cos\theta\rangle$ stabilizes close to the peak value. **(d)** For $E = -0.127$a.u. and the two laser has a frequency separation of $2\omega_{IR}$, $\langle\cos\theta\rangle$ (black line) oscillates around zero and vanishes as the IR is turned off. Similar results apply to any phase delays.

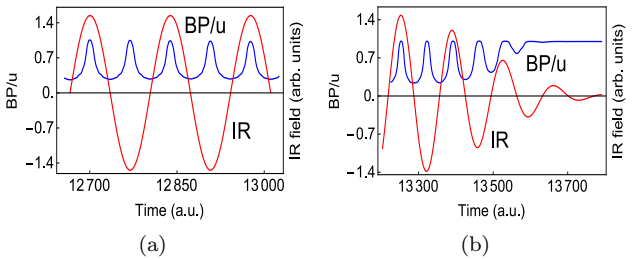

FIG. 7. (Color online) The bound population (BP) of electrons ($\langle\psi_{e1}(t)|\hat{P}|\psi_{e1}(t)\rangle$). The plot (blue curve) is normalized by the final bound population (u= $\langle\psi_{e1}|\psi_{e1}\rangle$). The peak is going lower due to ionization. The launch energy $E = -0.082$a.u.. The red curve is the IR field. **(a)** The IR is on. **(b)** The IR is being turned off.

or vice versa), which contributes to a nonzero integral. In Fig. 5, four different launch energies are picked. Each line records the orientation in terms of the phase delay. The oscillation of each line indicates that the surviving electrons' angular distribution switches between the upper and lower half sphere when continuously tuning the phase delay. Since the energy transfer from the IR to the electron (after excited) mostly happens at the first few IR cycles [5], the time of the electron being excited (controlled by phase delay) becomes crucial in determining the phase of the electron wave packets trapped at the quasi-stable states. As a result, tuning the phase delay will change the orientation, as indicated by Eq. 11. Figure 5 also reveals different phase delay dependence for varied launch energies. The below threshold behavior, shown by Fig. 5(a) and 5(b), has inverted phase delay dependence with respect to the above threshold behavior, shown by Fig. 5(d). However, they are not inverted with respect to Fig. (5c), and more study is needed to understand this contrary result.

We want to check the angular symmetry while the IR is still on. In the following discussion, we use the quantity $\langle\Psi_e(\vec{r},t)|\cos\theta|\Psi_e(\vec{r},t)\rangle$, which is time dependent since the IR is still on. First, $\langle\cos\theta\rangle$ is oscillating in time while the IR is on, as depicted by the black lines in Fig. 6(a) and Fig. 6(b). The cases shown in Fig. 6(a) and 6(b) have the same launch energy $E = -0.082a.u.$. They have inverted angular distribution because their phase delays differ by $\pi/2$, which match the results in Fig. 5. The peak in the black line repeats every half of one IR cycle and follows the IR intensity. Also, when we smoothly turn off the IR field, $\langle\cos\theta\rangle$ stops oscillating and stabilizes near the peak value, as depicted in Fig. 6(c). In order to find the reason, we calculate $\langle\psi_{e1}(t)|\hat{P}|\psi_{e1}(t)\rangle$ as a function of time, where $\hat{P}$ is an projection operator to all bound states. Figure 7(a) reveals that the population of bound electrons also oscillates periodically while the IR is on. During each IR cycle, the electrons experience ionization and combination twice due to the ponderomotive motion, which is the reason for the periodical oscillation of $\langle\cos\theta\rangle$. As the IR is being turned off, shown in Fig. 7(b), the population of bound electrons stabilizes, which is the final amount of electrons that survive the IR laser. This amount of electrons contributes both to the maximal of $\langle\cos\theta\rangle$ while the IR is on and the stable value of it when the IR is off, as shown in Fig. 6(c).

Second, the final stable value of the orientation does not depend on the time of turning off the IR. Figure 6(c) shows the behavior of the orientation when the IR is being turned off at time $t = 13.5 \times 10^3$a.u.. Similar behavior is observed when we turn off IR at other longer or shorter times, although the survival population varies. As a final point, we also calculate $\langle\cos\theta\rangle$ for $N = 2$. As expected, a symmetrical distribution ($\langle\cos\theta\rangle \sim 0$) is obtained for any phase delay. Fig. 6(d) shows that $\langle\cos\theta\rangle$ (black line) oscillates about zero while the IR is on and goes to zero when it is off. The magnitude of oscillation is approximately an order smaller than that in Fig. 6(c).

IV. CONCLUSION

Quasi-stability of highly excited atoms in a strong field have been extensively discussed in the past fifty years [12–14]. Various mechanisms of stabilization and many related experiments can be found [15–20]. The fact that Rydberg atoms have lower chance to absorb energy keeps the electron bound for a relatively long time. Those

surviving electrons, besides the same principal quantum number, tend to have the same even or odd (depending on the initial energy) angular quantum numbers [10]. Thus, a coherent effect is expected if electrons are being excited from different laser sources. The UV-pulse-train can be divided into two components, and they could separately act as a source, contributing electrons to the quasi-stable states.

In conclusion, we have studied the quasi-stability of UV-pulse-train-excited atoms in a strong IR field. When the two frequencies are separated by two IR photons, the survival probability will be a coherent superposition of the two contributions. By tuning the phase delay between the IR and the UV-pulse-train, we can coherently modulate the probability. The same coherence in the survival probability is not expected if the frequency separation is only one IR photon, where the survival probability is an incoherent addition of the two contributions. However, an asymmetry of the electron's angular distribution is observed in this case. By evaluating the orientation, we show the symmetry is oscillating as a function of the phase delay. And interestingly, the value of $\langle\cos\theta\rangle$ oscillates periodically in time while the IR is on. The period is half the IR cycle, and it stablizes after the IR is turned off. The oscillation of $\langle\cos\theta\rangle$ is due to the electrons experiencing recombination and ionization in each IR period, which is an interesting picture of quasi-stability in strong IR fields. With the growing techniques of attosecond physics [21], faster laser control and more accurate detection become possible. The above discussed coherence and angular distribution should be detectable in the lab. When studying pulse-train-excited atoms, the coherent effect shown above is surely of great importance to consider.

The author thanks Baochun Yang and Hua-Chieh Shao for helpful discussions. This work was supported by the U.S. Department of Energy, Office of Science, Basic Energy Sciences, under Award No. DE-SC0012193.

[1] M. W. Noel, W. M. Griffith, and T. F. Gallagher, Phys. Rev. Lett. **83**, 1747 (1999).
[2] A. Arakelyan and T. F. Gallagher, Phys Rev. A **87**, 023410 (2013).
[3] A. Arakelyan, T. Topcu, F. Robicheaux, and T. F. Gallagher, Phys. Rev. A **90**, 013413 (2014).
[4] J. H. Gurian, K. R. Overstreet, H. Maeda, and T. F. Gallagher, Phys. Rev. A **82**, 043415 (2010).
[5] E. S. Shuman, R. R. Jones, and T. F. Gallagher, Phys. Rev. Lett. **101**, 263001 (2008).
[6] R. R. Jones, D. W. Schumacher, and P. H. Bucksbaum, Phys. Rev. A **47**, R49 (1993).
[7] P. Johnsson, R. López-Martens, S. Kazamias, J. Mauritsson, C. Valentin, T. Remetter, K. Varjú, M.B. Gaarde, Y. Mairesse, H. Wabnitz, P. Saliéres, Ph. Balcou, K. J. Schafer, and A. L'Huillier, Phys. Rev. Lett. **95**, 013001 (2005).
[8] Vincent Carrat, E. Magnuson, and T. F. Gallagher, Phys. Rev. A **92**, 063414 (2015).
[9] K. J. Schafer, Mette B. Gaarde, Arne Heinrich, Jens Biegert, and Ursula Keller, Phys. Rev. Lett. **92**, 023003 (2004).
[10] Changchun Zhong, F. Robicheaux, Phys, Rev. A. **92**, 013406 (2015).
[11] F. Robicheaux, J. Phys. B **45**, 135007 (2012).
[12] W. C. Henneberger, Phys. Rev. Lett. **21**, 838 (1968).
[13] M. Pont, N. R. Walet, M. Gavrila, and C. W. McCurdy, Phys. Rev. Lett. **61**, 939 (1988).
[14] J. H. Eberly and K. C. Kulander, Science **262**, 1229 (1993).
[15] K. C. Kulander, K. J. Schafer, and J. L. Krause, Phys. Rev. Lett. **66**, 2601 (1991).
[16] M. V. Fedorov and A. Movsesian, J. Phys. B **21**, L155 (1988).
[17] H. G. Muller, Phys. Rev. Lett. **83**, 3158 (1999).
[18] U. Eichmann, A. Saenz, S. Eilzer, T. Nubbemeyer, and W. Sandner, Phys. Rev. Lett. **110**, 203002 (2013).
[19] R. R. Jones and P. H. Bucksbaum, Phys. Rev. Lett. **67**, 3215 (1991).
[20] L. D. Noordam, H. Stapelfeldt, D. I. Duncan, and T. F. Gallagher, Phys. Rev. Lett. **68**, 1496 (1992).
[21] Ferenc Krausz and Misha Ivanov, Rev of Mod. Phys. **81**, 163 (2009).